International Journal of Nanomedicine

ISSN: (Print) (Online) Journal homepage: www.tandfonline.com/journals/dijn20

Cerium oxide NPs mitigate the amyloid formation of α-synuclein and associated cytotoxicity

Zahra Zand, Pegah Afarinesh Khaki, Abbas Salihi, Majid Sharifi, Nadir Mustafa Qadir Nanakali, Asaad AB Alasady, Falah Mohammad Aziz, Koorosh Shahpasand, Anwarul Hasan & Mojtaba Falahati

To cite this article: Zahra Zand, Pegah Afarinesh Khaki, Abbas Salihi, Majid Sharifi, Nadir Mustafa Qadir Nanakali, Asaad AB Alasady, Falah Mohammad Aziz, Koorosh Shahpasand, Anwarul Hasan & Mojtaba Falahati (2019) Cerium oxide NPs mitigate the amyloid formation of α-synuclein and associated cytotoxicity, International Journal of Nanomedicine, , 6989-7000, DOI: 10.2147/IJN.S220380

To link to this article: https://doi.org/10.2147/IJN.S220380

© 2019 Zand et al.

Published online: 29 Aug 2019.

Submit your article to this journal

Article views: 233

View related articles

View Crossmark data

Citing articles: 14 View citing articles

Full Terms & Conditions of access and use can be found at
https://www.tandfonline.com/action/journalInformation?journalCode=dijn20

International Journal of Nanomedicine

Dovepress

open access to scientific and medical research

Open Access Full Text Article

ORIGINAL RESEARCH

Cerium oxide NPs mitigate the amyloid formation of α-synuclein and associated cytotoxicity

This article was published in the following Dove Press journal:
International Journal of Nanomedicine

Zahra Zand[1,*]
Pegah Afarinesh Khaki[2,*]
Abbas Salihi[3,4]
Majid Sharifi[5,6]
Nadir Mustafa Qadir Nanakali[7,8]
Asaad AB Alasady[9]
Falah Mohammad Aziz[3]
Koorosh Shahpasand[10]
Anwarul Hasan[11,12]
Mojtaba Falahati[5]

[1]Department of Biochemistry and Biophysics, Faculty of Advanced Science and Technology, Tehran Medical Sciences, Islamic Azad University, Tehran, Iran; [2]Department of Molecular Genetics, Faculty of Advanced Science and Technology, Tehran Medical Sciences, Islamic Azad University, Tehran, Iran; [3]Department of Biology, College of Science, Salahaddin University-Erbil, Kurdistan Region, Iraq; [4]Department of Medical Analysis, Faculty of Science, Tishk International University, Erbil, Iraq; [5]Department of Nanomedicine, Faculty of Advanced Science and Technology, Tehran Medical Sciences, Islamic Azad University, Tehran, Iran; [6]Department of Animal Science, Faculty of Agriculture, University of Tabriz, Tabriz, Iran; [7]Department of Biology, College of Science, Cihan University-Erbil, Kurdistan Region, Iraq; [8]Department of Biology, College of Education, Salahaddin University-Erbil, Kurdistan Region, Iraq; [9]Anatomy, Biology and Histology Unit, College of Medicine, University of Duhok, Kurdistan Region, Iraq; [10]Department of Brain and Cognitive Sciences, Cell Science Research Center, Royan Institute for Stem Cell Biology and Technology, ACECR, Tehran, Iran; [11]Department of Mechanical and Industrial Engineering, College of Engineering, Qatar University, Doha 2713, Qatar; [12]Biomedical Research Center, Qatar University, Doha 2713, Qatar

*These authors contributed equally to this work

Correspondence: Mojtaba Falahati
Department of Nanomedicine, Faculty of Advanced Science and Technology, Tehran Medical Sciences, Islamic Azad University, Tehran, Iran
Email mojtaba.falahati@alumni.ut.ac.ir

Anwarul Hasan
Department of Mechanical and Industrial Engineering, College of Engineering, Qatar University, Doha 2713, Qatar
Email hasan.anwarul.mit@gmail.com

Aim: Among therapeutic proposals for amyloid-associated disorders, special attention has been given to the exploitation of nanoparticles (NPs) as promising agents against aggregation.

Methods: In this paper, the inhibitory effect of cerium oxide (CeO_2) NPs against α-synuclein (α-syn) amyloid formation was explored by different methods such as Thioflavin T (ThT) and 8-anilinonaphthalene-1-sulfonic acid (ANS) fluorescence spectroscopy, Congo red adsorption assay, circular dichroism (CD) spectroscopy, transmission electron microscopy (TEM), and bioinformatical approaches. Also, the cytotoxicity of α-syn amyloid either alone or with CeO_2 NPs against neuron-like cells (SH-SY5Y) was examined using 3-(4,5-dimethylthiazol-2-yl)-2,5-diphenyltetrazolium bromide (MTT), flow cytometry, and quantitative real-time polymerase chain reaction (Bax and Bcl-2 gene expression) assays.

Results: ThT and ANS fluorescence assays indicated that CeO_2 NPs inhibit the formation of aggregated species and hydrophobic patches of α-syn in amyloidogenic conditions, respectively. Congo red and CD assays demonstrated that CeO_2 NPs reduce the formation of amyloid species and β-sheets structures of α-syn molecules, respectively. TEM investigation also confirmed that CeO_2 NPs limited the formation of well-defined fibrillary structures of α-syn molecules. Molecular docking and dynamic studies revealed that CeO_2 NPs could bind with different affinities to α-syn monomer and amyloid species and fibrillar structure of α-syn is disaggregated in the presence of CeO_2 NPs. Moreover, cellular assays depicted that CeO_2 NPs mitigate the cell mortality, apoptosis, and the ratio of Bax/Bcl-2 gene expression associated with α-syn amyloids.

Conclusion: It may be concluded that CeO_2 NPs can be used as therapeutic agents to reduce the aggregation of proteins and mitigate the occurrence of neurodegenerative diseases.

Keywords: cerium oxide, nanoparticle, amyloid, cytotoxicity, spectroscopy, cellular assay, inhibition

Introduction

In neurodegenerative diseases such as Alzheimer's disease (AD), Parkinson's disease, and Huntington's disease, abnormal changes in specific protein structures cause their aggregation and subsequent accumulation in nerve cells, which can destroy neurons.[1] One of the most important neuronal proteins is α-synuclein (α-syn) that their aggregations result in formation of Lewy body filaments associated with impaired nerve functioning.[2] Indeed, these filaments are heterogeneous and rich in β-sheet structures along with hydrophobicity and tinctorial attributes.[3] The α-syn filaments stimulate high cytotoxicity by increasing reactive oxygen species (ROS) and altering or damaging the structure of the nerve cells through apoptosis.[4,5] The most important factors affecting α-

© 2019 Zand et al. This work is published and licensed by Dove Medical Press Limited. The full terms of this license are available at https://www.dovepress.com/terms.php and incorporate the Creative Commons Attribution – Non Commercial (unported, v3.0) License (http://creativecommons.org/licenses/by-nc/3.0/). By accessing the work you hereby accept the Terms. Non-commercial uses of the work are permitted without any further permission from Dove Medical Press Limited, provided the work is properly attributed. For permission for commercial use of this work, please see paragraphs 4.2 and 5 of our Terms (https://www.dovepress.com/terms.php).

syn fibrillation are: 1) structural factors including modification of hydrophilic headgroups and hydrophobic tails, changing surface charge of protein, presence of aromatic amino acids, and 2) environmental factors including changes of pH, high temperature, protein concentration, oxidative stress, and the peptide chain mutations.[6] α-Syn is the most common protein in the nervous system with 140 amino acids (14 kDa) that consist 1% of the total protein in the cytosolic region of the brain.[7] Hence, to stop the growth and accumulation of α-syn in nerve cells, various methods such as organic or non-organic compounds, small peptides, and gene therapy have been exploited.[8] In this field, due to the enormous impact of nanoscience on medical and therapeutic services, the effect of nanomaterials on controlling the aggregation of α-syn has been given special attention. Unlike gold (Au) nanoparticles (NPs) that induce α-syn fibrillation by influencing both the nucleation and growth phases,[9] iron NPs,[10] and even carbon NPs[11] have been shown to prevent the formation of Aβ fibrillation. Besides, it has been revealed that titanium dioxide (TiO_2) NPs cause α-syn fibrillation, whereas silicon oxide (SiO_2) NPs and Tin oxide (SnO_2) NPs do not affect α-syn fibrillation.[12] While, Wu, Wang, Sun, Xue[13] previously demonstrated that SiO_2 NPs cause α-syn aggregation through induction of oxidative stress.

Therefore, the effects of nanomaterials on protein aggregation are not fully understood, and conflicting results have been reported about inhibitory effects of NPs against protein fibrillation. Also, the application of NPs as therapeutic agents is still obscure due to cytotoxic variation based on their physicochemical properties.[14,15] Cerium oxide (CeO_2) NPs shows antioxidant features derived from their superoxide dismutase (SOD)- and catalase (CAT)-like activities in vitro and in vivo.[16] In general, CeO_2 NPs due to the surface self-regeneration, which depends on redox-cycling between Ce^{3+} and Ce^{4+} conditions,[17] and vacancy of oxygen in the lattice structure,[18] can be used in medical activities to remove ROS. Although, the experiments showed that CeO_2 NPs could have antioxidant features;[19,20] the lack of CeO_2 NPs in the human body limits their use in biomedical applications due to the probable occurrence of systematic toxicity.[21] Hence, in this study, the inhibitory effects of CeO_2 NPs against the amyloid formation of α-syn were investigated by different spectroscopic and bioinformatical approaches. Afterwards, the cytotoxicity of α-syn amyloid either alone or in the presence of CeO_2 NPs was studied against SH-SY5Y cells.

Materials and methods

Materials

α-Syn, Thioflavin T (ThT), 8-anilinonaphthalene-1-sulfonic acid (ANS), Congo red, Dulbecco's Modified Eagle Medium/Nutrient Mixture F-12 (DMEM: F12), fetal bovine serum (FBS), L-glutamine, penicillin, streptomycin, and MTT were purchased from Sigma Co. (St. Louis, MO, USA). CeO_2 NPs, purity: 99.97%, APS: 10–30 nm, SSA: 30–50 m^2/g, bulk density: ~0.8–1.1 g/cm^3, and true density: 7.132 g/cm^3 were purchased from US Research Nanomaterials, Inc. (Houston, USA) and well characterized by different approaches in our previous paper.[22]

Methods

CeO_2 NP preparation

CeO_2 NPs with defined concentration was freshly solubilized in 1% (v/v) DMSO/water, sonicated for 30 mins by a sonicator probe (Misonix-S3000, USA) and were kept at ambient temperature. To reveal that NPs do not compromise ThT, Tyr, Congo red, and circular dichroism (CD) signals, all experiments were performed in the presence of probes and NPs concentrations in agreement with those of diluted solutions employed to examine aggregation.

Preparation of fibrils of α-syn

The α-syn amyloid samples (maximum concentration of 100 μM) were prepared by dissolving α-syn monomer in HEPES (pH 7.4, 20 mM, 150 mM NaCl) at 37°C at 700 rev/min based on the reported paper.[23] To monitor the impact of CeO_2 NPs on protein aggregation, α-syn samples with a single fixed concentration of CeO_2 NPs (40 μg/mL) (as the highest dose which does not show agglomeration) were co-incubated during the preparation of fibrils of α-syn.

ThT fluorescence assay

All fluorescence spectroscopy assays were performed using a Cary Eclipse VARIAN fluorescence spectrophotometer (Varian, CA, USA). Amyloid kinetics was read using ThT as an extrinsic fluorescence probe. The fluorescence intensity was read at regular time intervals with λex and λem at 440 and 480 nm, respectively. Average of the fluorescence intensity of three samples was considered to plot the kinetic study. After dilution of protein samples to 3 μM in the HEPES buffer and addition of ThT solution (15 μM), the kinetic graph was plotted. Afterwards, a sigmoidal fit was used to calculate the kinetic parameters of α-syn amyloid either alone or with CeO_2 NPs based on

the reported equations in previous reports.[24,25] Briefly, apparent growth rate constant (kapp) and lag phase time were calculated to be $1/\tau$ and $t_0-2\ \tau$, respectively, where t_0 is the time needed to show 50% of the maximal emission intensity and τ is nonlinear regression.[24,25]

ANS fluorescence assay

The ANS fluorescence study was done to monitor the structural changes of α-syn species. Aliquots of the α-syn samples either alone or co-incubated with fixed concentration of CeO_2 NPs were removed at 100 hrs and diluted to a final concentration of 3 μM in HEPES buffer (20 mM, pH 7.4) containing 20 μM ANS. The excitation wavelength with a slit width of 10 nm was fixed at 380 nm, and emission wavelength with a slit width of 5 nm was scanned between 400 and 600 nm.

Congo red binding assay

The experiment was done at room temperature using a Cary Eclipse VARIAN absorbance (Varian, CA, USA) spectroscopy. Briefly,10 μM of the α-syn amyloid samples either alone or co-incubated with a single dose of CeO_2 NPs for 100 hrs was added to Congo red solution with a concentration of 20 μM and the absorbance signals were read between 400 and 600 nm.

Far-UV CD measurement

Ellipticity changes of protein samples were monitored employing an AVIV 215 spectropolarimeter (Proterion Corp., USA). Aliquots of the α-syn samples either alone or co-incubated with a single dose of CeO_2 NPs after 100 hrs were diluted to a final concentration of 10 μM in HEPES buffer (20 mM, pH 7.4). Afterwards, the ellipticity changes were read in the range of 190–260 nm and the percent of the secondary structure of protein samples were calculated using CDNN software (Proterion Corp., USA).

Transmission electron microscopy (TEM) investigation

The morphology of α-syn amyloid either alone or with CeO_2 NPs was captured using TEM machine with a model of EM10C (Zeiss, 100 KV, Germany). Briefly, 15 μL of protein samples was dropped to a carbon-coated grid and left at room temperature for 15 mins. Afterwards, the morphology of aggregated species was studied using TEM investigation.

Simulation methods

Two spherical CeO_2 clusters of diameters 3 and 2 nm were constructed by repeating the unit cells of CeO_2 crystal and used in the docking and the molecular dynamics simulations, respectively. A ligand-binding study was carried out using HEX 6.3 software.[26] The molecular dynamic simulations were done using the Forcite code and the universal force field.[27] All force filed parameters were set to default.

Cell culture

SH-SY5Y cells were obtained from Royan institute and were cultured in DMEM-F12 medium containing FBS (10%), streptomycin (100 μg/mL), penicillin (100 U/mL), and incubated at 37°C in a 5% CO_2. 1×10^4 cells/well were seeded into 96-well plate and the α-syn samples removed from samples incubated either alone or with a single dose of CeO_2 NPs (40 μg/mL) under amyloidogenic environment added to the cells with a final concentration of 10 μM for protein and 4 μg/mL for NPs and incubated for 24 hrs. Cells exposed to 20 mM HEPES buffer (pH 7.4) were considered as negative control samples.

MTT assay

MTT stock solutions with a concentration of 5 mg/mL were then added to samples for 4 hrs followed by aspiration and addition of DMSO. Finally, the optical density of samples was read at 570 nm using an ELISA reader (Expert 96, Asys Hitch, Ec Austria). Data were reported as the percentage of MTT reduction in comparison with the negative control cells, assuming that the optical density of the negative control cells was 100%.

Flow cytometry assay

Cell apoptosis and necrosis tests were conducted by flow cytometry with Annexin V-FITC Apoptosis Staining Kit (ab14085, UK) based on the manufacturer's protocol. Briefly, after treatment of cells with an aliquot of α-syn in the absence or presence of CeO_2 with a final concentration of 10 μM for 24 hrs, cells were harvested, washed, resuspended in 500 μL of binding buffer, added by 5 μL of Annexin V-FITC for 15 mins in the dark, and added by 10 μL of PI. Afterwards, cell apoptosis and necrosis were analyzed by flow cytometry (FACS Calibur, BD Biosciences, San Jose, CA 95131-1807. USA) with flow 6.3 software.

Real time gene expression assay

The expression amount of (BCL-2) and BAX genes was estimated by real-time PCR analysis based on our previous paper.[28] TRIzol reagent (Thermo Fisher Scientific, Waltham, MA, USA) and RevertAid first-strand cDNA synthesis kit (Takara, Japan) were used to extract total

RNA and synthesis of cDNA, respectively according to the manufacturer's instructions. The quantitative real-time polymerase chain reaction (qPCR) assay was done using an ABI Step One Sequence Detection System (Thermo Fisher Scientific) by SYBR® Premix Taq™ II (Takara, Japan) using GAPDH as a control.

Statistical analysis

Data were reported as mean ± standard deviation (SD) from three independent experiments. The statistical analysis was carried out using one-way ANOVA. The significance of data was considered as $*P \leq 0.05$.

Results

Characterization of NPs

It was depicted that CeO_2 NPs show an average diameter of around 30 nm with a vibration peak at 738 cm^{-1}.[22] Indeed, potential transport of therapeutic agents like NPs into the human brain is one of the most demanding tasks in anti-amyloid drug development owing to the blood-brain barrier (BBB). To go across the BBB, the size of NPs as one of the most important factors must be considered. Actually, NPs with a size of less than 50 nm have been shown to provide a well-dispersed state in working solutions, cross the BBB and may provide promising anti-amyloid functions.[29,30]

ThT fluorescence assay

Fibrillization investigation of the α-syn was done either alone or with CeO_2 NPs at a fixed concentration of 40 μg/mL. The fibrillization process was detected by using ThT fluorescence experiment. The aggregation studies exhibited the features of a representative amyloid fibril plot: a sigmoidal curve with a beginning lag process, where no enhance of fluorescence intensity is detected, because no amyloid species are produced, a quick fibrillation process, where the fluorescence signal enhances as the amyloid species form, and a steady-state process, where the maximum fluorescence intensity does not change significantly. Figure 1A shows the fibrillization plot for the α-syn either alone or with CeO_2 NPs. Table 1 reveals that the lag phase time in the absence of NPs is around 23 hrs, however, it increases to 35.5 hrs in the presence of NPs. Indeed, the free α-syn depicts no fibrillization till 23 hrs, and NP impact is determined in the lag phase time range. In the case of α-syn co-incubated with CeO_2 NPs, the presence of the NPs increases the duration of lag phase time and inhibits the fibrillization process. Also, a reduction in k_{app} was observed in the presence of NPs (Table 1), which suggests the reaction kinetic in the presence of CeO_2 NPs is quite slower than those in the absence of NPs.

ANS fluorescence assay

The amyloid forms of protein are typically distinguished from their monomer species through binding to ANS probe. The partial denaturation of the natively disordered proteins like α-syn and transformation into amyloid structures induces the formation of hydrophobic patches which can bind ANS molecules. This binding leads to an enhancement in ANS fluorescence intensity and a blue shift in λex.[31] A comparison of ANS emission intensities of α-syn species (monomer, amyloid either alone or with CeO_2 NPs) is depicted in Figure 1B. As anticipated, the spectra of α-syn monomer and ANS exhibited negligible ANS fluorescence intensity. At amyloid states, the ANS intensity of α-syn was ~3.5 times more than that of monomer species, indicating increased induction of hydrophobic moieties. Besides, the binding of ANS to α-syn in the amyloid state led to a significant blue shift in λ_{max} (Figure 1B). However, a reduction in ANS fluorescence intensity of α-syn amyloid was observed when α-syn monomer co-incubated with CeO_2 NPs during amyloidogenic conditions. The reduction in ANS fluorescence intensity of α-syn amyloid was distinguishable in the presence of CeO_2 NPs. Protein in monomer state showed the maximum intensity of ANS fluorescence at around 500 nm, which decreased to 488 nm and 490 for α-syn amyloid alone and with CeO_2 NPs, respectively. The maximum ANS fluorescence intensity and pronounced blue shift may reveal that amyloid fibril species of α-syn is probably formed. However, co-incubation of α-syn with CeO_2 NPs may inhibit the formation of these amyloid species.

Congo red assay

Congo red assay was performed to evaluate the amyloid fibril formation of α-syn either alone or with CeO_2 NPs. Figure 1C depicts the Congo red absorbance of α-syn in different states. As can be seen, Congo red absorbance and blue shift for α-syn amyloid were highest among all states. However, Figure 1C reveals that Congo red absorbance and blue shift values in α-syn amyloid with CeO_2 NPs were lower than the maximum values for α-syn amyloid in the absence of CeO_2 NPs. Therefore, the amyloid formation of α-syn in amyloidogenic conditions was effectively inhibited by CeO_2 NPs.

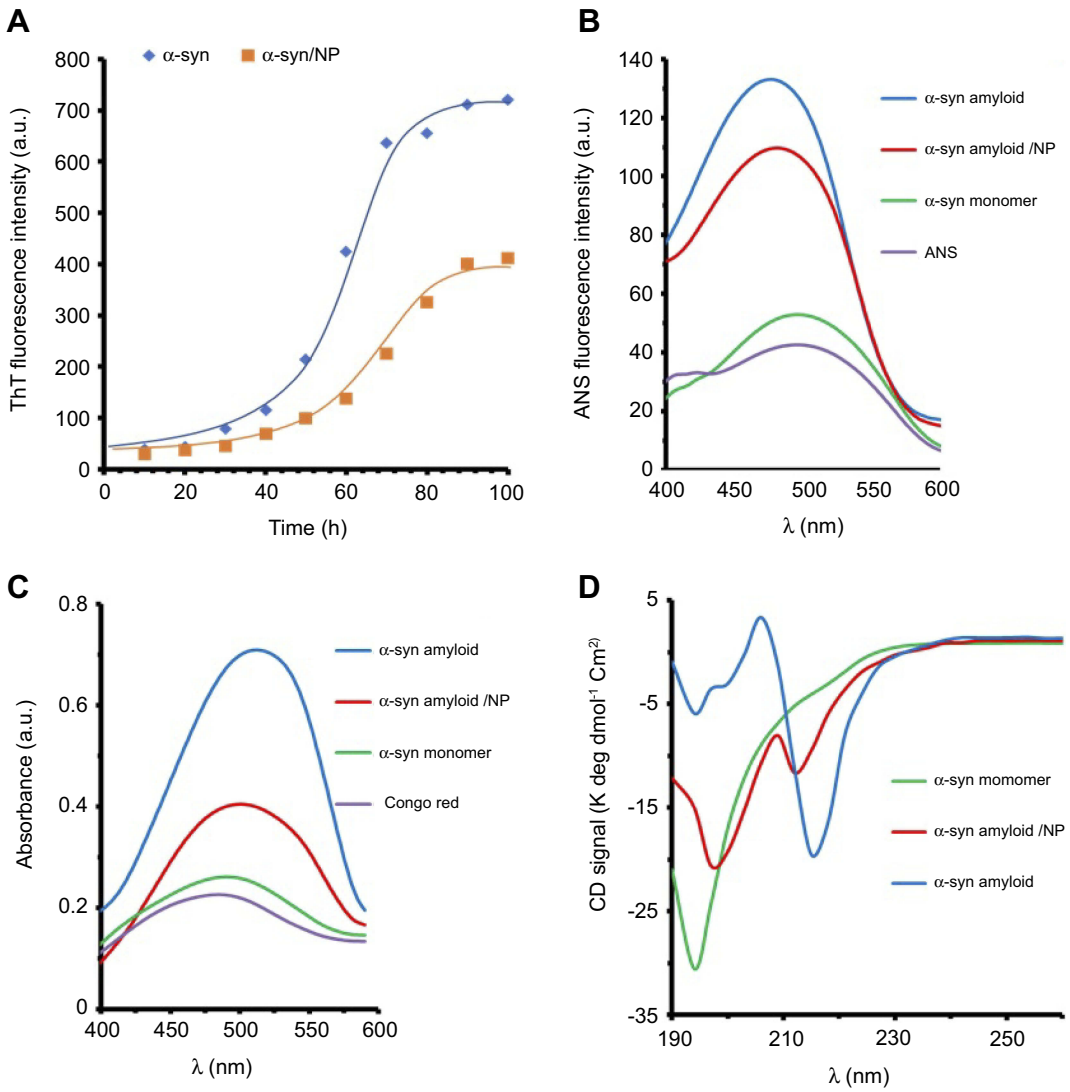

Figure 1 Spectroscopic studies of α-sync species either alone or co-incubated with CeO_2 NPs.
Notes: (**A**) Kinetic graph of α-syn fibrillation in the absence and presence of CeO_2 NPs based on ThT assay; (**B**) ANS fluorescence intensity of different species of α-syn; (**C**) Congo red absorbance of different species of α-syn; and (**D**) CD spectra of different species of α-syn.
Abbreviations: CeO_2, cerium oxide; NPs, nanoparticles; ThT, thioflavin T; ANS, anilinonaphthalene-1-sulfonic acid; α-syn, α-synuclein; CD, circular dichroism.

Table 1 Influence of CeO_2 NPs on the kinetics parameters of **α**-syn fibrillization calculated by ThT fluorescence assay

Samples	(Kapp) (h^{-1})	Lag time (hrs)	Amplitude (a.u.)
α-syn	0.062	23	721
α-syn/CeO_2 NPs	0.058	35.5	412

Abbreviations: CeO2, cerium oxide; NPs, nanoparticles; α-syn, α-synuclein; ThT, Thioflavin T.

CD study

The ellipticity changes of a biomolecule in far-UV wavelength (190–250 nm) show a n→π* transition band around 220 nm and a π→π* transition band about 190 nm which arises from peptide bonds.[31] Therefore, CD signals of a biomolecule in this wavelength range can be used to determine the alteration in secondary structure of protein. Far-UV CD bands of different species of α-syn are shown in Figure 1D. α-Syn in monomer state exhibited a minimum at around 195 nm, indicating the dominant random coil conformation in protein structure. The content of secondary structure of α-syn is also tabulated in Table 2. However, for α-syn in the amyloid state, the minima at 195 nm were almost disappeared and shifted toward higher wavelength

value around 217 nm, indicating remarkable loss of random coil structure and acquisition of β-sheet-like structures.[31] Afterwards, to explore the inhibitory effect of CeO_2 NPs on amyloid formation, we performed CD experiment for α-syn amyloid/CeO_2 NP complex. Changing the ellipticity values was found in the α-syn amyloid samples co-incubated with CeO_2 NPs, where β-sheet-like structures were profoundly lower than that of amyloid state without NPs (Table 2). A decrease in the content of β-sheet-like structures suggesting that α-syn preserve its secondary structure to some extent in the presence of CeO_2 NPs. Indeed, in comparison to the monomer state of α-syn, where the random coil structure was calculated to be 73.7%, this structure decreased to 19.4% at amyloidogenic condition. However, the secondary structure (% random coil) of α-syn is largely preserved in the presence of CeO_2 NPs.

TEM investigation

TEM study was exploited to observe the morphology of aggregated species. Figure 2 displays TEM images of α-syn monomer as control or incubated for 100 hrs under amyloidogenic conditions either alone or with CeO_2 NPs. As shown in Figure 2A, α-syn monomer does not show any observable aggregated species. Figure 2B demonstrates mature amyloids with typical amyloid fibrils. However, in α-syn samples incubated with 40 μg/mL CeO_2 NPs, generation of such aggregated species with amyloid fibrils morphology were considerably inhibited, with the formation of amorphous appearance (Figure 2C). In other words, in the presence of CeO_2 NPs, the well-defined amyloid structures with amyloid fibrils morphology were lost to view, and instead, amorphous aggregates with different sizes were appeared (Figure 2C). This study also provides interesting data regarding the inhibitory effect of CeO_2 NPs against the amyloid formation.

Molecular docking study

The NMR structure of α-syn (PDB ID: 1XQ8) and α-syn fibrils (PDB ID: 2N0A) were downloaded from the online Protein Data Bank RCSB PDB (http://www.pdb.org). The molecular docking was executed with the larger spherical cluster of CeO_2 (Figure 3). The calculated binding energy for CeO_2 nanocluster with α-syn fibrils (Figure 3A) and α-syn monomer (Figure 3B) was −141.98 and −199.35 E-value, respectively. Indeed, it may be suggested that the affinity of CeO_2 nanocluster to α-syn monomer is more than α-syn fibrils. Visualization of the binding site was performed by using CHIMERA (www.cgl.ucsf.edu/chimera) and PyMOL (http://pymol.sourceforge.net/) tools, as shown in Figure 3C. As can be seen in Figure 3C, the most attractive residues of α-syn fibrils are Ala-76, Val-77, Ala-90, Ala-89, and Ile-88. However, for α-syn monomer, the most attractive sites are Met-1, Asp-2, Met-5, Lys-6, Ser-8 (Figure 3D).

Table 2 The structural characteristics of **α**-syn at different states

Protein sate	Random coil %	α-helix %	β-sheet %	Turn and loop %
Monomer	73.7	11.9	4.5	9.9
Amyloid	19.4	7.5	61.3	11.8
Amyloid/CeO_2 NP	38.9	11.3	39.4	10.4

Abbreviations: α-syn, α-synuclein; CeO2, cerium oxide; NP, nanoparticle.

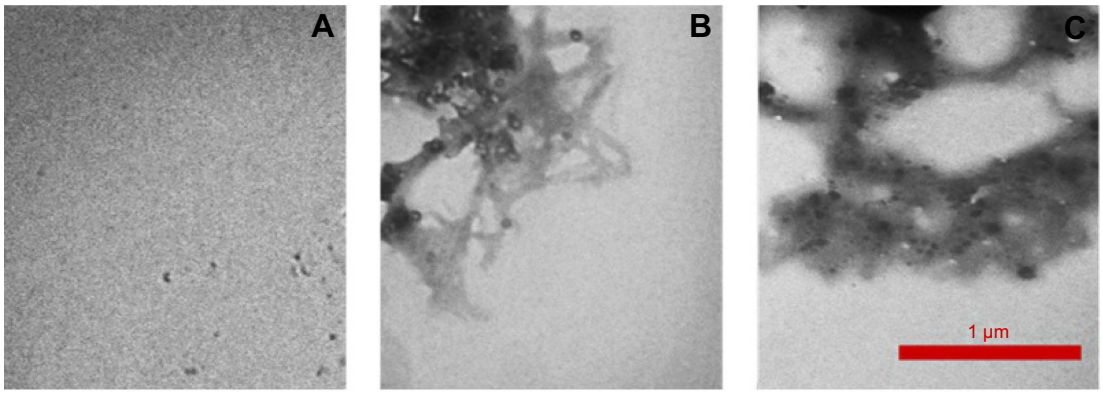

Figure 2 TEM images of different species of **α**-syn.
Notes: (**A**) α-syn monomer; (**B**) α-syn amyloid; and (**C**) α-syn amorphous aggregates in the presence of CeO_2 NPs.
Abbreviations: TEM, transmission electron microscopy; α-syn, α-synuclein; CeO_2, cerium oxide; NPs, nanoparticles.

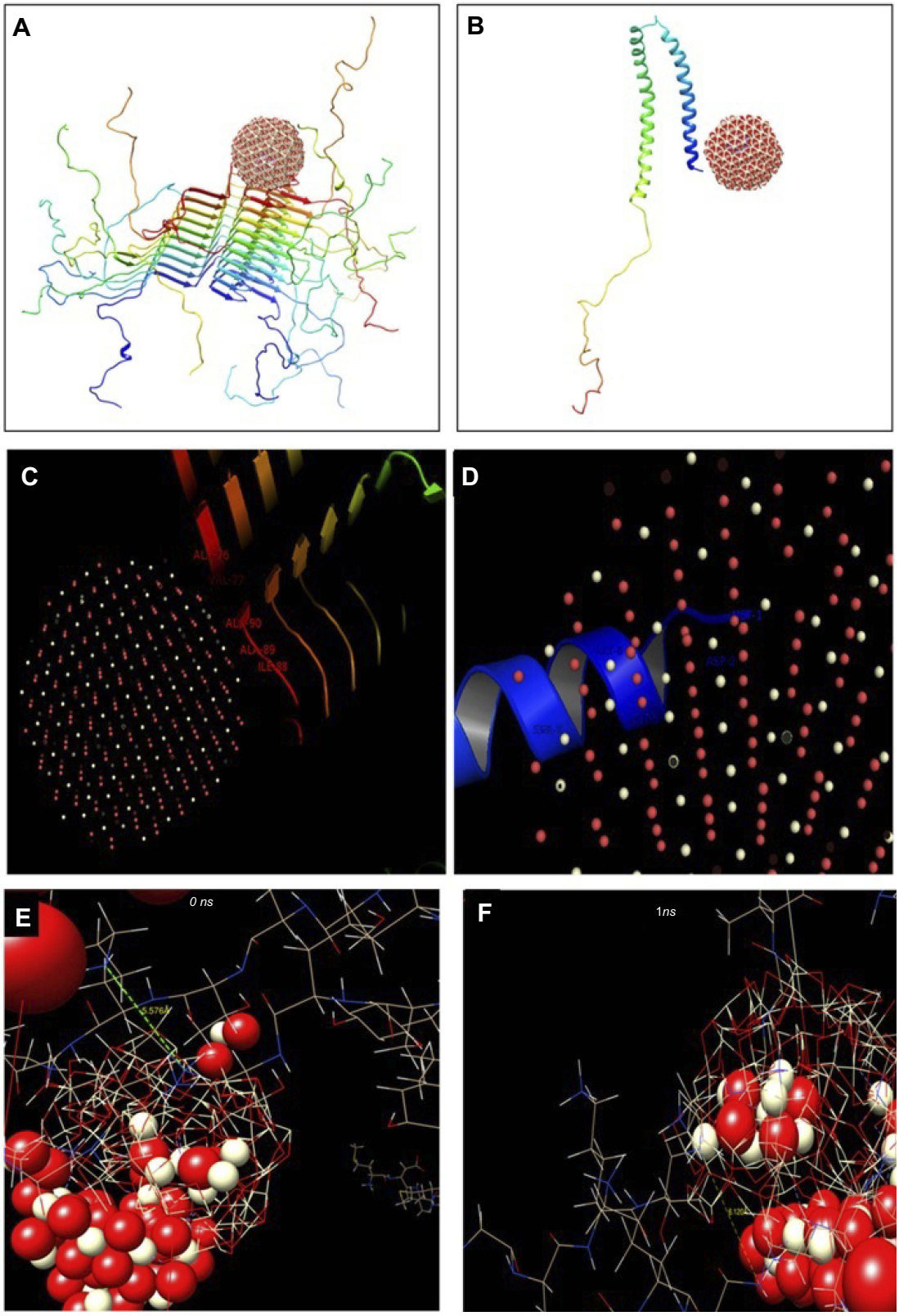

Figure 3 Theoretical studies of interaction between CeO_2 nanocluster and different species of α-syn.
Notes: (**A**) Molecular docking of CeO_2 nanocluster with α-syn fibrils; (**B**) molecular docking of CeO_2 nanocluster with α-syn monomer; (**C**) visualization of docked pose of CeO_2 nanocluster with α-syn fibrils; (**D**) visualization of docked pose of CeO_2 nanocluster with α-syn monomer; (**E**) the conformation of α-syn amyloid in the beginning; and (**F**) and after 1 ns evolution exploited by molecular dynamic study.
Abbreviations: CeO_2, cerium oxide; α-syn, α-synuclein.

Therefore, it may be identified that as Ala, Val, and Ile are hydrophobic residues, the interaction of CeO_2 nanocluster with α-syn amyloid is done through hydrophobic forces. However, due to the dominant hydrophilic residues (Asp, Lys, Ser) in the binding site of the α-syn monomer with CeO_2 nanocluster, the hydrophilic interaction such as electrostatic forces and hydrogen binding is mostly involved in the complex formation between nanocluster and α-syn in the monomer state.

Molecular dynamics study

Molecular modeling was carried out to explore the conformational changes of α-syn in the presence of CeO_2 NPs. Two α-syn amyloid structures and five clusters of CeO_2 were covered by water molecules. The NVE ensemble with a time step of 1 fs was exploited in the molecular modeling simulation. The conformation of α-syn amyloid in the beginning and after 1 ns evolution was exhibited in (Figure 3E and F). As can be observed, the neighboring protein chains have a distance of 5.576 Å at the beginning of the simulation (Figure 3E). However, this distance increased to 6.120 Å in the presence of CeO_2 NPs, indicating that the amyloid structure of α-syn is partially disaggregated (Figure 3F). These data are in good agreement with our spectroscopic outcomes which showed an inhibitory effect of CeO_2 NPs against the amyloid formation of α-syn.

MTT assay

MTT assay was done to investigate the toxicity of aggregated species of α-syn either alone or with CeO_2 NPs. As shown in Figure 4, α-syn monomer with a concentration of 10 μM and CeO_2 NPs with a concentration of 4 μg/mL do not trigger significant toxicity against SH-SY5Y cells after 24 hrs. However, incubating cells with α-syn amyloid with a concentration of 10 μM trigger significant toxicity against cells, which reduce the cell viability to 29.08±5.36% (***P<0.00, relative to negative control cells). Afterwards, it was seen that incubating cells with α-syn amyloid/NP complex with the same concentration, recovered the cell viability to 59.79±10.27% ($^{\#}P$<0.05, relative to α-syn amyloid-treated cells). These data indicated that formed aggregates in the presence of CeO_2 NPs are significantly less toxic in comparison with α-syn amyloids in the absence of NPs.

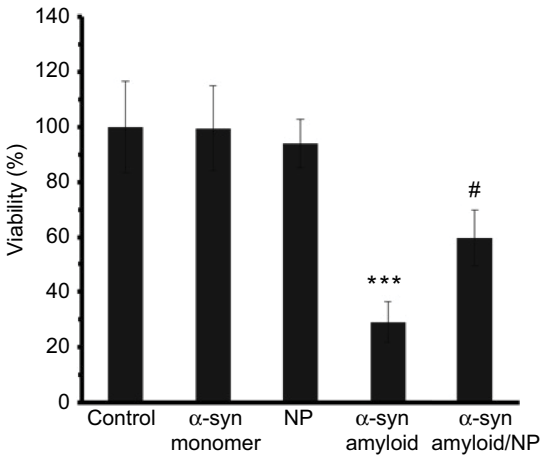

Figure 4 MTT assay of different species of α-syn and CeO_2 NPs.
Notes: ***P-value <0.001 relative to control sample; $^{\#}P$-value <0.05 relative to α-syn amyloid sample.
Abbreviations: α-syn, α-synuclein; CeO_2, cerium oxide; NPs, nanoparticles.

Flow cytometry analysis

Cultured SH-SY5Y cells were treated with 10 μM of α-syn amyloid either alone or with CeO_2 NPs and flow cytometry analysis was done to quantify the apoptosis and necrosis. As displayed in Figure 5A, control cells show no significant apoptosis or necrosis. However, α-syn amyloid significantly increased the percent of early apoptosis (22.2%, **P<0.01), late apoptosis (16.7%, ***P<0.001), and necrosis (7.0%, **P<0.01) relative to the control group (Figure 5B) In another side, α-syn amyloid co-incubated with CeO_2 NPs showed higher level of viability and reduced amount of early apoptosis (7.5%, $^{\#\#}P$<0.01), late apoptosis (6.6%, $^{\#\#}P$<0.01), and necrosis (3.9%, $^{\#}P$<0.05) relative to α-syn amyloid-treated group, suggesting the inhibiting role of CeO_2 NPs against induced cytotoxicity by α-syn amyloids (Figure 5C).

Real-time PCR

qPCR was also employed to investigate the mRNA levels of apoptotic markers (Bcl-2, and Bax) in SH-SY5Y cells exposed to α-syn samples incubated with or without CeO_2 NPs for 100 hrs. Data indicated that the mRNA expression of these apoptotic genes was markedly changed in SH-SY5Y cells due to α-syn amyloid exposure. While no increase in relative ratio of Bax/Bcl-2 mRNA level was observed for control samples, relative ratio of Bax/Bcl-2 mRNA level increased significantly after 24 hrs exposure to α-syn amyloid fibrils (*P<0.05) (Figure 6). However, in the present of CeO_2 NPs, the relative ratio of Bax/Bcl-2 mRNA level was reduced to 1.28±0.11% ($^{\#}P$<0.05)

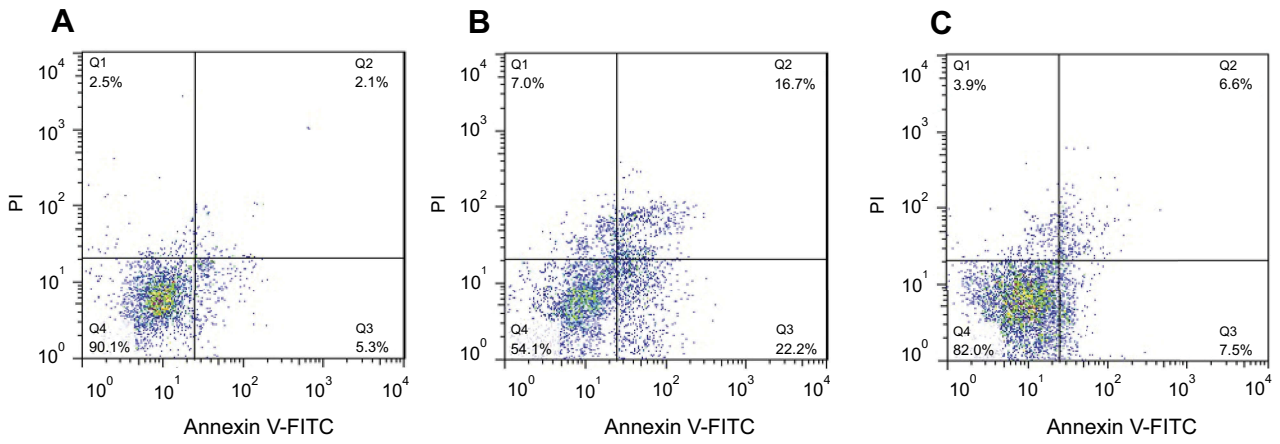

Figure 5 SH-SY5Y cell apoptosis and necrosis after being exposed to, (**A**) negative control group, (**B**) aliquots of **α**- syn amyloid formed in the absence of CeO_2 NPs, and (**C**) aliquots of **α**- syn amyloid formed in the presence of CeO_2 NPs (**C**).
Abbreviations: α-syn, α-synuclein; CeO_2, cerium oxide; NPs, nanoparticles.

(Figure 6), indicating that formed aggregated species are relatively less toxic compared to α-syn amyloids in the absence of NPs.

Discussion

Recent studies by Mohammad-Beigi et al,[32] revealed that the different shape of α-syn fibrils is formed after aggregation due to the difference in β-sheet folding, the molecular accumulation between the sheets levels and the interaction of lateral chains in the environment. Indeed, even slight variations in environmental conditions such as changes in pH, temperature, ions concentration, nano-objects concentrations, and drug concentrations can strongly affect the aggregation and folding processes of α-syn. Therefore, by identifying any of the factors and their effects on the accumulation of α-syn, in addition to predicting the different forms of aggregation, it is possible to prevent the α-syn accumulation. One of the most effective factors in reducing α-syn aggregation is the reduction of the ROS that can be achieved by the activity of antioxidant enzymes. In this regard, Murakami et al,[33] showed that depletion of the activity of SOD in mice increases the accumulation of amyloid plaques. In this line, CeO_2 NPs are considered to be an appropriate option for preventing the accumulation of amyloids due to the SOD and CAT-like properties.[34] In this study, we have exhibited that CeO_2 NPs may be one of the environmental factors that reduce the accumulation of α-syn amyloid fibrils. In agreement with our findings, Cimini et al,[35] determined that the CeO_2 NPs modified with PGE and anti-Aβ, in addition to the detection of amyloid Aβ, reduced their aggregation connected with the antioxidant properties of CeO_2 NPs. Analogously, in the cortical neurons cell model isolated from Sprague–Dawley rat embryos, Dowding et al,[36] using CeO_2 NPs could prevent mitochondrial fragmentation and cell death by decreasing the level of Aβ-amyloid derived from peroxidase and peroxynitrite-like properties. At the same time, it was found that the use of CeO_2 NPs reduces the rate of development of AD relied on the reduction of amyloid levels through peroxidase-like activity.[37] In this line, Kaushik, Bharadwaj, Kumar, Wei[3] in a computational model showed that CeO_2 NPs, based on their antioxidant properties could be used as a potential inhibitor of α-Syn accumulation. Whereas, Sekar, Kumar, Mukherjee, Chandrasekaran[38] reported that CeO_2 NPs play a promoting role in the formation of HSA fibrillation via the enhancement of β-sheet structures in protein conformation.

Besides, in the present study, it was observed that CeO_2 NPs at 40 μg/mL could increase the lag phase time of α-syn fibrillation, indicating a decrease in fibrillation levels. This finding, in concurrence with the findings of John et al,[39] described that Au NPs with polymeric coatings and small molecules inhibit amyloid accumulation by increasing the lag phase time. On the other hand, our cellular results indicate that CeO_2 NPs can have a significant effect on the survival of host cells in the presence of toxic species of α-syn amyloid. We found that CeO_2 NPs reduce cytotoxicity by decreasing α-syn accumulation. In this regard, conflicting reports are due to the type of NPs and protein. A group of NPs increase protein aggregation and cytotoxicity, and others with antioxidant activity or surface modification decrease protein accumulation and

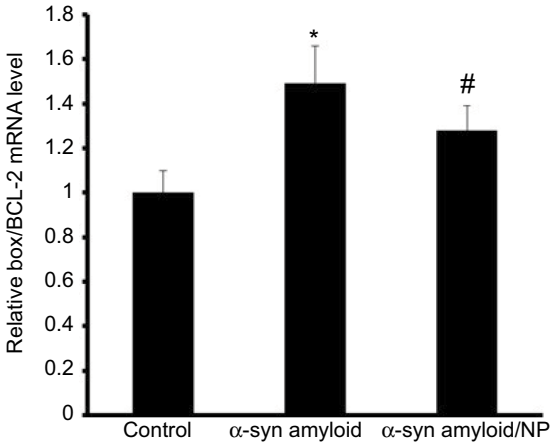

Figure 6 Changes in the Bax/Bcl-2 ratio (of the mRNA levels) in all treated cases relative to control group.
Notes: *P-value <0.05 relative to control sample; #P-value <0.05 relative to α-syn amyloid sample.
Abbreviation: α-syn, α-synuclein.

their assosiated cytotoxicity. For example, Mandal, Debnath, Jana, Jana[40] showed that by modifying the surface of Au NPs with trehalose, the amount of protein aggregation decreases, and hence cytotoxicity is greatly reduced. While, it has been shown that the interaction of insulin with zinc oxide NPs results in the structural reconstruction of amyloid clusters and associated cytotoxicity.[41] Nevertheless, Samai, Basu, Mati, Bhattacharya[42] recently used bare CeO_2 NPs, CeO_2 NPs coated with folic acid (CeO_2-FA NPs), and CeO_2 NPs coated with polyacrylic acid (CeO_2-PAA NPs) to prevent the aggregation of lysosomes and amyloid growth. Their results revealed that not only the highest amyloid aggregation blockage was related to CeO_2-PAA NPs and CeO_2-FA NPs compared to bare CeO_2 NPs, but also significantly reduced the level of cytotoxicity relative to the control group. Therefore, with the change of surface charge from positive to negative by some coatings, the level of protein aggregation or amyloid-fibrillation along with cytotoxicity can be greatly reduced. In this regard, Javdani, Rahpeyma, Ghasemi, Raheb[43] exhibited that the change in the surface charge of iron NPs from positive to negative by dextran would reduce amyloid-fibrillation in both β-amyloids and α-syn.

Conclusion

In the present study, CeO_2 NPs were shown to inhibit the formation of α-syn amyloid fibrils- associated cytotoxicity against SH-SY5Y cells. Spectroscopic and theoretical studies demonstrated that CeO_2 NPs bind to α-syn monomer and increase the lag phase time of amyloid fibril formation. Also, it was shown that the aggregated species formed by α-syn with CeO_2 NPs are relatively less toxic compared to amyloid fibrils formed in the absence of CeO_2 NPs. These outcomes hold a great promise for helping in tackling the challenges related to the therapeutic efficiency of NPs in neurodegenerative diseases.

Acknowledgment

This article was made possible by the grant GCC-2017-005 under the GCC collaborative research Program from Qatar University, and the grant by Islamic Azad University of Tehran Medical Sciences, Tehran, Iran. All statements in the article are sole responsibility of the authors.

Disclosure

The authors report no conflicts of interest in this work.

References

1. Marei HE, Althani A, Lashen S, Cenciarelli C, Hasan A. Genetically unmatched human iPSC and ESC exhibit equivalent gene expression and neuronal differentiation potential. *Sci Rep*. 2017;7(1):17504–17510. doi:10.1038/s41598-017-17882-1
2. Wills J, Credle J, Haggerty T, Lee J-H, Oaks AW, Sidhu A. Tauopathic changes in the striatum of A53T α-synuclein mutant mouse model of Parkinson's disease. *PLoS One*. 2011;6(3):e17953–9. doi:10.1371/journal.pone.0017953
3. Kaushik AC, Bharadwaj S, Kumar S, Wei D-Q. Nano-particle mediated inhibition of Parkinson's disease using computational biology approach. *Sci Rep*. 2018;8(1):9169–9179. doi:10.1038/s41598-018-27580-1
4. Jiang T, Sun Q, Chen S. Oxidative stress: a major pathogenesis and potential therapeutic target of antioxidative agents in Parkinson's disease and Alzheimer's disease. *Prog Neurobiol*. 2016;147:1–19. doi:10.1016/j.pneurobio.2016.07.005
5. Elmann A, Telerman A, Ofir R, Kashman Y, Lazarov O. β-amyloid cytotoxicity is prevented by natural achillolide A. *J Nat Med*. 2018;72(3):626–631. doi:10.1007/s11418-018-1191-0

6. Fink AL. The Aggregation and fibrillation of α-synuclein. *Acc Chem Res*. 2006;39(9):628–634. doi:10.1021/ar050073t
7. Adamczyk A, Solecka J, Strosznajder J. Expression of a-synuclein in different brain parts. *J Physiol Pharmacol*. 2005;56(1):29–37.
8. Panza F, Lozupone M, Logroscino G, Imbimbo BP. A critical appraisal of amyloid-β-targeting therapies for Alzheimer disease. *Nat Rev Neurol*. 2019;1:1–10.
9. Alvarez YD, Fauerbach JA, Pellegrotti JV, Jovin TM, Jares-Erijman EA, Stefani FD. Influence of gold nanoparticles on the kinetics of alpha-synuclein aggregation. *Nano Lett*. 2013;13(12):6156–6163. doi:10.1021/nl403490e
10. Mahmoudi M, Hosseinkhani H, Hosseinkhani M, et al. Magnetic resonance imaging tracking of stem cells in vivo using iron oxide nanoparticles as a tool for the advancement of clinical regenerative medicine. *Chem Rev*. 2011;111(2):253–280. doi:10.1021/cr1001832
11. Padmanabhan P, Kumar A, Kumar S, Chaudhary RK, Gulyas B. Nanoparticles in practice for molecular-imaging applications: an overview. *Acta Biomater*. 2016;41:1–16. doi:10.1016/j.actbio.2016.06.003
12. Mohammadi S, Nikkhah M. TiO2 nanoparticles as potential promoting agents of fibrillation of α-synuclein, a parkinson's disease-related protein. *Iran J Biotechnol*. 2017;15(2):87–97. doi:10.15171/ijb.1519
13. Wu J, Wang C, Sun J, Xue Y. Neurotoxicity of silica nanoparticles: brain localization and dopaminergic neurons damage pathways. *ACS Nano*. 2011;5(6):4476–4489. doi:10.1021/nn103530b
14. Naz S, Beach J, Heckert B, et al. Cerium oxide nanoparticles: a 'radical'approach to neurodegenerative disease treatment. *Nanomedicine*. 2017;12(5):545–553. doi:10.2217/nnm-2016-0399
15. Paul A, Hasan A, Rodes L, Sangaralingam M, Prakash S. Bioengineered baculoviruses as new class of therapeutics using micro and nanotechnologies: principles, prospects and challenges. *Adv Drug Del Rev*. 2014;71:115–130. doi:10.1016/j.addr.2014.01.004
16. Korsvik C, Patil S, Seal S, Self WT. Superoxide dismutase mimetic properties exhibited by vacancy engineered ceria nanoparticles. *Chem Commun (Camb)*. 2007;10:1056–1058. doi:10.1039/b615134e
17. Dahle JT, Arai Y. Environmental geochemistry of cerium: applications and toxicology of cerium oxide nanoparticles. *Int J Environ Res Public Health*. 2015;12(2):1253–1278. doi:10.3390/ijerph120201253
18. Sayle TX, Parker SC, Catlow CR. The role of oxygen vacancies on ceria surfaces in the oxidation of carbon monoxide. *Surface Science*. 1994;316(3):329–336.
19. Asati A, Santra S, Kaittanis C, Nath S, Perez JM. Oxidase-like activity of polymer-coated cerium oxide nanoparticles. *Angew Chem*. 2009;48(13):2308–2312. doi:10.1002/anie.200805279
20. Karakoti A, Singh S, Dowding JM, Seal S, Self WT. Redox-active radical scavenging nanomaterials. *Chem Soc Rev*. 2010;39(11):4422–4432. doi:10.1039/b919677n
21. Xu C, Qu X. Cerium oxide nanoparticle: a remarkably versatile rare earth nanomaterial for biological applications. *NPG Asia Mater*. 2014;6(3):90–99. doi:10.1038/am.2013.88
22. Eskandari N, Babadaei MMN, Nikpur S, et al. Biophysical, docking, and cellular studies on the effects of cerium oxide nanoparticles on blood components: in vitro. *Int J Nanomedicine*. 2018;13:4575–4585. doi:10.2147/IJN.S172162
23. González-Lizárraga F, Socías SB, Ávila CL, et al. Repurposing doxycycline for synucleinopathies: remodelling of α-synuclein oligomers towards non-toxic parallel beta-sheet structured species. *Sci Rep*. 2017;7:41755. doi:10.1038/srep41755
24. Cabaleiro-Lago C, Szczepankiewicz O, Linse S. The effect of nanoparticles on amyloid aggregation depends on the protein stability and intrinsic aggregation rate. *Langmuir*. 2012;28(3):1852–1857. doi:10.1021/la203078w
25. Mahdavimehr M, Meratan AA, Ghobeh M, Ghasemi A, Saboury AA, Nemat-Gorgani M. Inhibition of HEWL fibril formation by taxifolin: mechanism of action. *PLoS One*. 2017;12(11):0187841–49. doi:10.1371/journal.pone.0187841
26. Ritchie DW, Venkatraman V. Ultra-fast FFT protein docking on graphics processors. *Bioinformatics*. 2010;26(19):2398–2405. doi:10.1093/bioinformatics/btq444
27. Rappé AK, Casewit CJ, Colwell K, Goddard WA III, Skiff WM. UFF, a full periodic table force field for molecular mechanics and molecular dynamics simulations. *J Am Chem Soc*. 1992;114(25):10024–10035. doi:10.1021/ja00051a040
28. Babadaei MMN, Moghaddam MF, Solhvand S, et al. Biophysical, bioinformatical, cellular, and molecular investigations on the effects of graphene oxide nanosheets on the hemoglobin structure and lymphocyte cell cytotoxicity. *Int J Nanomedicine*. 2018;13:6871–6877. doi:10.2147/IJN.S174048
29. Hanada S, Fujioka K, Inoue Y, Kanaya F, Manome Y, Yamamoto K. Cell-based in vitro blood–brain barrier model can rapidly evaluate nanoparticles' brain permeability in association with particle size and surface modification. *Int J Mol Sci*. 2014;15(2):1812–1825. doi:10.3390/ijms15021812
30. Shilo M, Sharon A, Baranes K, Motiei M, Lellouche J-PM, Popovtzer R. The effect of nanoparticle size on the probability to cross the blood-brain barrier: an in-vitro endothelial cell model. *J Nanobiotechnology*. 2015;13(1):19–29. doi:10.1186/s12951-015-0075-7
31. Qadeer A, Rabbani G, Zaidi N, Ahmad E, Khan JM, Khan RH. 1-Anilino-8-naphthalene sulfonate (ANS) is not a desirable probe for determining the molten globule state of chymopapain. *PLoS One*. 2012;7(11):e50633. doi:10.1371/journal.pone.0050633
32. Mohammad-Beigi H, Hosseini A, Adeli M, et al. Mechanistic understanding of the interactions between nano-objects with different surface properties and α-synuclein. *ACS Nano*. 2019;1:1–10.
33. Murakami K, Murata N, Noda Y, et al. SOD1 (copper/zinc superoxide dismutase) deficiency drives amyloid beta protein oligomerization and memory loss in mouse model of Alzheimer disease. *J Biol Chem*. 2011;286(52):44557–44568. doi:10.1074/jbc.M111.279208
34. Dowding JM, Dosani T, Kumar A, Seal S, Self WT. Cerium oxide nanoparticles scavenge nitric oxide radical (NO). *Chem Commun (Camb)*. 2012;48(40):4896–4898. doi:10.1039/c2cc30485f
35. Cimini A, D'Angelo B, Das S, et al. Antibody-conjugated PEGylated cerium oxide nanoparticles for specific targeting of Aβ aggregates modulate neuronal survival pathways. *Acta Biomater*. 2012;8(6):2056–2067. doi:10.1016/j.actbio.2012.01.035
36. Dowding JM, Song W, Bossy K, et al. Cerium oxide nanoparticles protect against Aβ-induced mitochondrial fragmentation and neuronal cell death. *Cell Death Differ*. 2014;21(10):1622–1632. doi:10.1038/cdd.2014.72
37. Seal S, Das S, Cimini A, D'angelo B. Nanoparticles of cerium oxide targeted to an amyloid beta antigen of alzheimer's disease and associated methods. *Google Pat*. 2016;1:1.2.
38. Sekar G, Kumar NP, Mukherjee A, Chandrasekaran N. Cerium oxide nanoparticles promote HSA fibrillation in vitro. *Int J Biol Macromol*. 2017;103:1138–1145. doi:10.1016/j.ijbiomac.2017.05.180
39. John T, Gladytz A, Kubeil C, Martin LL, Risselada HJ, Abel B. Impact of nanoparticles on amyloid peptide and protein aggregation: a review with a focus on gold nanoparticles. *Nanoscale*. 2018;10(45):20894–20913. doi:10.1039/c8nr04506b
40. Mandal S, Debnath K, Jana NR, Jana NR. Trehalose-functionalized gold nanoparticle for inhibiting intracellular protein aggregation. *Langmuir*. 2017;33(49):13996–14003. doi:10.1021/acs.langmuir.7b02202
41. Asthana S, Hazarika Z, Nayak PS, et al. Insulin adsorption onto zinc oxide nanoparticle mediates conformational rearrangement into amyloid-prone structure with enhanced cytotoxic propensity. *Biochim Biophys Acta Gen Subj*. 2019;1863(1):153–166. doi:10.1016/j.bbagen.2018.10.004
42. Samai B, Basu A, Mati SS, Bhattacharya SC. Antiamyloid activity of functionalized cerium oxide nanoparticle on lysozyme fibrillation: spectroscopic and microscopic investigation. *Materialia*. 2019;6:100285–100295. doi:10.1016/j.mtla.2019.100285
43. Javdani N, Rahpeyma SS, Ghasemi Y, Raheb J. Effect of superparamagnetic nanoparticles coated with various electric charges on α-synuclein and β-amyloid proteins fibrillation process. *Int J Nanomedicine*. 2019;14:799–808. doi:10.2147/IJN.S190354

International Journal of Nanomedicine

Dovepress

Publish your work in this journal

The International Journal of Nanomedicine is an international, peer-reviewed journal focusing on the application of nanotechnology in diagnostics, therapeutics, and drug delivery systems throughout the biomedical field. This journal is indexed on PubMed Central, MedLine, CAS, SciSearch®, Current Contents®/Clinical Medicine, Journal Citation Reports/Science Edition, EMBase, Scopus and the Elsevier Bibliographic databases. The manuscript management system is completely online and includes a very quick and fair peer-review system, which is all easy to use. Visit http://www.dovepress.com/testimonials.php to read real quotes from published authors.

Submit your manuscript here: https://www.dovepress.com/international-journal-of-nanomedicine-journal